THE JOURNAL OF PHYSICAL CHEMISTRY A

 VOLUME 107, NUMBER 14, APRIL 10, 2003

ARTICLES

Photolysis of Oxalyl Chloride $(ClCO)_2$ at 248 nm: Emission of CO($v' \leqslant 3$, $J' \leqslant 51$) Detected with Time-Resolved Fourier Transform Spectroscopy

Chia-Yan Wu and Yuan-Pern Lee*

Department of Chemistry, National Tsing Hua University, 101, Sec. 2, Kuang Fu Road, Hsinchu 30013, Taiwan

J. F. Ogilvie

Escuela de Quimica, Universidad de Costa Rica, San Pedro, San Jose, Costa Rica

Niann S. Wang

Department of Applied Chemistry, National Chiao Tung University, 1001, Ta Hsueh Road, Hsinchu 30010, Taiwan

Received: October 18, 2002

Upon photolysis of oxalyl chloride at 248 nm, rotationally resolved emission of CO ($v \leq 3$) in the spectral region 1900−2300 cm^{-1} was detected with a step-scan time-resolved Fourier transform spectrometer under nearly collisionless conditions. Boltzmann-like rotational distributions of CO ($v = 1$ and 2) correspond to temperatures ~2290 ± 100 and 1910 ± 130 K, respectively, with average rotational energy of 16 ± 2 kJ mol^{-1}; several lines of CO ($v = 3$) were also observed, but their weak intensity precludes quantitative analysis. The average vibrational energy of CO is estimated to be 10 ± 3 kJ mol^{-1} according to observed vibrational populations of $v = 1$ and 2 and that of $v = 0$ and 3 predicted with surprisal analysis. Combining the average internal energy of CO determined in this work and average translational energies of photofragments Cl, CO, and ClCO determined previously by Suits and co-workers, we derived a revised energy balance. We observed no emission of ClCO near 1880 cm^{-1}, indicating that ClCO ($v_1 = 1$) decomposes rapidly and that surviving ClCO has little vibrational excitation in the CO stretching mode. Most CO produced from decomposition of ClCO is in its vibrational ground state with small rotational excitation, undetectable with our technique.

Introduction

Oxalyl chloride, $(ClCO)_2$, has recently been characterized as an excellent source of chlorine atoms for kinetic studies because it has a relatively large absorption cross section at 193 nm with a quantum yield of Cl atoms ~2.00 and because the other final product CO is unreactive.[1]

Early physical−chemical investigations focused on conformational properties of $(ClCO)_2$; the trans conformation is the most stable.[2,3,4] UV irradiation of $(ClCO)_2$ isolated in solid Ar or Xe led to photoinduced isomerization and, in solid Xe, formation of CO and phosgene (Cl_2CO).[5] Ahmed et al. investigated the photodissociation dynamics of $(ClCO)_2$ near 235 nm with a photofragment imaging technique.[6] Images of photofragments Cl*($^2P_{1/2}$), Cl ($^2P_{3/2}$), and CO ($v = 0$) in various rotational levels were recorded via resonance-enhanced mul-

* To whom correspondence should be addressed. Jointly appointed by the Institute of Atomic and Molecular Sciences, Academia Sinica, Taipei, Taiwan. E-mail: yplee@mx.nthu.edu.tw. Fax: 886-3-5722892.

10.1021/jp0222550 CCC: $25.00
Published on Web 03/14/2003

tiphoton ionization (REMPI) to yield distributions of their translational energy. The recoil speed distribution of Cl* exhibits a dominant rapid component with a translational energy distribution peaking at ~48 kJ mol^{-1}, whereas that of Cl shows two components with a dominant slow component peaking at ~10 kJ mol^{-1} and a rapid minor component similar to Cl*. These rapid components of both Cl and Cl*, and the higher rotational levels of CO, show anisotropic angular distributions, whereas distributions for slow fragments are nearly isotropic. On the basis of these observations, Ahmed et al.[6] suggested that the photodissociation proceeds via an impulsive three-body mechanism yielding translationally rapid Cl* and Cl, rapid and rotationally excited CO, and slow chloroformyl radical (ClCO); most ClCO undergoes subsequent dissociation to yield CO with little rotational energy and Cl, both with little translational energy release.

Hemmi and Suits further investigated this system at 193 nm with photofragment translational spectroscopy by employing for ionization the tunable VUV light from an undulator beamline of a synchrotron.[7] They observed that translational energy distributions of Cl and CO are bimodal, whereas the distribution for ClCO has a single sharp maximum with an abrupt lack of population for translational energies less than ~3 kJ mol^{-1}, confirming that much ClCO product undergoes secondary dissociation to form Cl and CO.[6] The observed translational energy release of Cl and CO upon photolysis of $(ClCO)_2$ at 193 nm is similar to that at 235 nm.

Although experiments of photofragment translational spectroscopy yield detailed information on kinematics of dissociation, they provide little information on the internal-energy distribution of CO. The distribution of CO reported by Ahmed et al.[6] based on REMPI spectra indicates that the rotational distribution of CO ($v = 0$) has a maximum at $J \cong 30$ and extends beyond $J = 50$; the total integrated signal for CO ($v = 1$) is less than 5% of that for CO ($v = 0$), indicating negligible vibrational excitation of CO. On the basis of their experimental results, Ahmed et al. derived a total energy release on photodissociation of $(ClCO)_2$ at 235 nm ~26 kJ mol^{-1} greater than available energy calculated from corresponding enthalpies of formation; they proposed that the discrepancy might be accounted for if some ClCO remains bound.

The step-scan time-resolved Fourier transform spectroscopy (TR−FTS) provides much improved resolution and sensitivity over conventional IR emission techniques.[8,9] Following photodissociation of haloethene at 193 nm, we observed vibration−rotationally resolved emission spectra of HX (X = F, Cl, or Br) and identified both three-center and four-center elimination channels for the first time.[10−12] Our results clearly demonstrate that a more nearly complete distribution of vibration−rotational levels can be determined with TR−FTS because of its multiplex advantage and the nature of IR emission. In contrast, observed vibration−rotational levels recorded in REMPI spectra might be limited by Franck−Condon factors or stability of intermediate states.[13−16] In this paper, we report observation of IR emission of CO ($v' \leq 3$) with TR−FTS upon photolysis of $(ClCO)_2$ at 248 nm; the energy balance for this process is revised.

Experiment

The apparatus employed to obtain time-resolved infrared emission spectra has been described previously;[8,9] only a summary is given here. The photolysis beam from a KrF laser (248 nm, Lambda Physik, LPX150) has dimensions ~2 × 10 mm^2 with energy reduced to ~11 mJ per pulse. A filter (OCLI, W05200−6X) passing 1670−2325 cm^{-1} was employed to facilitate undersampling to reduce the number of data points. The InSb detector has a rise time of ~0.7 μs; its signal was amplified with an effective bandwidth of 1 MHz before being digitized with an external data-acquisition board (PAD1232, 12-bit ADC) at 50-ns intervals. Data were averaged over 70 laser pulses at each scan step; 5034 scan steps were performed to yield an interferogram resulting in a CO emission spectrum with a resolution of 0.3 cm^{-1}. In one experiment, a resolution of 0.13 cm^{-1} was employed. Time-resolved spectra at 50-ns intervals were subsequently summed over various periods after photolysis to yield a spectrum with a signal-to-noise ratio suitable for quantitative analysis.

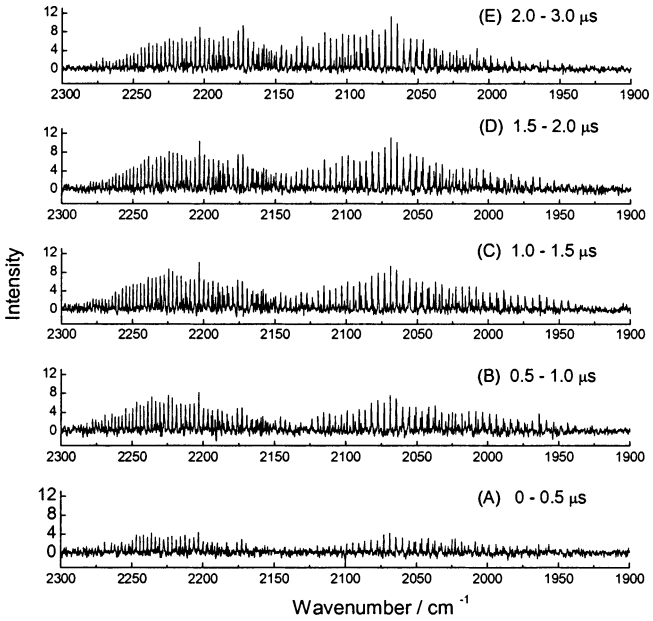

Figure 1. Infrared emission spectra of CO in the spectral region 2300−1900 cm^{-1} averaged for periods 0−0.5 (A), 0.5−1.0 (B), 1.0−1.5 (C), 1.5−2.0 (D), and 2.0−3.0 μs (E) after photolysis of $(ClCO)_2$ at 0.056 Torr and 298 K with a KrF laser at 248 nm. Resolution is 0.3 cm^{-1}; 70 laser pulses were averaged at each scan step. Four spectra recorded under similar conditions were averaged.

$(ClCO)_2$ (Lancaster, >98%) was used without purification except for degassing at 77 K. The pressure of $(ClCO)_2$ in the flow cell was kept below 0.056 Torr, and no buffer gas was added.

Results and Discussion

We employed a total pressure of 0.056 Torr to maintain nearly collisionless conditions within a ~1 μs period. The absorption cross section of $(ClCO)_2$ at 248 nm is ~3 × 10^{-19} cm^2;[1] hence, about 2% of $(ClCO)_2$ was dissociated upon irradiation. Spectra of the improved signal-to-noise ratio were obtained on averaging four sets of spectra recorded in separate experiments under similar conditions.

A. Spectral Assignments and Rotational Distribution of CO. Figure 1 shows emission spectra of CO, at 0.3 cm^{-1} resolution, that were averaged over 0−0.5, 0.5−1.0, 1.0−1.5, 1.5−2.0, and 2.0−3.0 μs after laser irradiation of $(ClCO)_2$ at 0.056 Torr. The small intensity in trace A reflects the temporal response of the detection system. As shown in trace E, rotational quenching becomes perceptible after ~2 μs. An expanded partial spectrum averaged over 0−1.0 μs is shown in Figure 2; assignments based on spectral parameters reported by Ogilvie et al.[17] are shown as stick bars. The spectrum clearly shows that the 0.3-cm^{-1} resolution is adequate to resolve most lines of $v' = 1$ and 2; emission from high rotational levels of CO

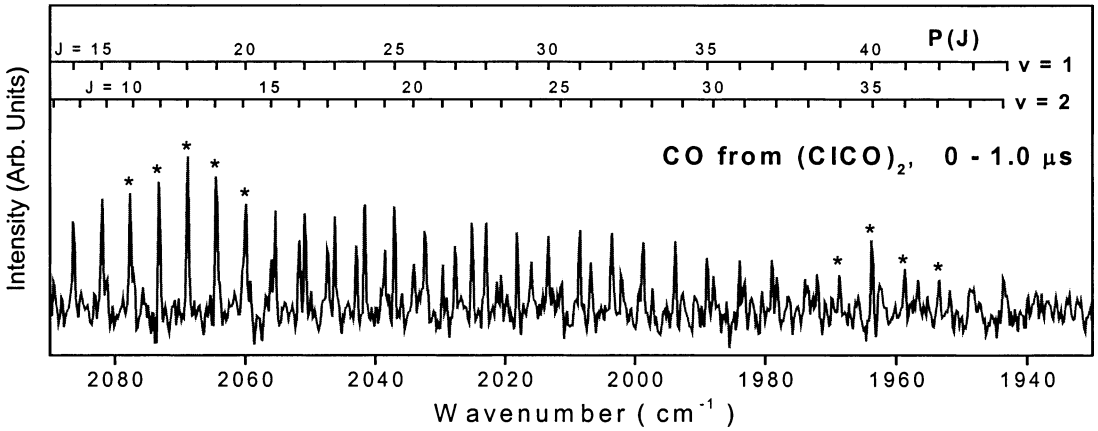

Figure 2. Partial infrared emission spectra of CO in the spectral region 2090−1930 cm^{-1} averaged for 0−1.0 μs after photolysis of $(ClCO)_2$ at 0.056 Torr and 298 K with laser light at 248 nm. Assignments are shown in stick diagrams; overlapped lines are indicated with *.

with J' up to 44 (P-branch) or 51 (R-branch) for $v' = 1$ and J' up to 39 for $v' = 2$ was observed.

We calculated values of the Einstein A coefficient according to this formula

$$A^{v'J'}_{v''J''} = \frac{16\pi^3\tilde{\nu}^3|\iota||\langle v'|p(R)|v''\rangle|^2\,(1 + C^{v'}_{v''}\,\iota + D^{v'}_{v''}\,\iota^2)}{3\epsilon_0 h(2J' + 1)}$$

in which $\langle v'|p(R)|v''\rangle$ is a pure vibrational matrix element of electric dipolar moment between vibrational states v' and v'', $\iota = {}^1/_2[J'(J' + 1) - J''(J'' + 1)]$ is a running number depending on rotational quantum numbers J' and J'', $C^{v'}_{v''}$ and $D^{v'}_{v''}$ are coefficients in the Herman-Wallis factor to take into account the rotational effect on the matrix element,[18] $\tilde{\nu}$ is the wavenumber of a transition from a vibration−rotational state (v', J') to another state (v'', J''), and ϵ_0 and h are fundamental constants. We employed calculated values of $C^{v'}_{v''}$ and $D^{v'}_{v''}$ consistent with a radial function p(R) derived from experimental values of vibration−rotational intensities of lines in absorption,[17] which were limited to values of J less than 33. Because the function for dipolar moment $p(R)$ shows satisfactory agreement with results from quantum computations well beyond its range of definition from experiment, and because we employed theoretical values of $C^{v'}_{v''}$ and $D^{v'}_{v''}$ instead of experimental values, which have in any case small magnitudes, Einstein coefficients calculated for J beyond 50 are expected to be reasonably reliable.

Each vibration−rotational line was normalized with the instrument response function, integrated, and divided by its respective Einstein coefficient to yield a relative population $P_v(J')$. To assess the effect of rotational quenching, we made semilogarithmic plots of $P_v(J')/(2J' + 1)$ of CO ($v' = 1$) for spectra obtained with integration periods 0−0.5, 0.5−1.0, 1.0−1.5, 1.5−2.0, and 2.0−3.0 μs and found Boltzmann-like rotational distributions corresponding to rotational temperatures of 2390 ± 180, 2250 ± 100, 2130 ± 90, 1850 ± 60, and 1440 ± 50 K, respectively; the uncertainties reflect one standard deviation in fitting. For $v' = 2$, fitted rotational temperatures are 2000 ± 170, 1850 ± 140, 1610 ± 120, 1380 ± 120, and 1050 ± 140 K, respectively, for spectra integrated over the same periods listed above. Considering possible experimental errors, we conclude that rotational quenching is negligible within 1.0 μs. Hence, we used spectra integrated over 0−1.0 μs for measurements of the nascent distribution. Semilogarithmic plots of $P_v(J')/(2J' + 1)$ vs $J'(J' + 1)$ for P and R branches of CO ($v' = 1$and 2) recorded for period 0−1.0 μs are shown in Figure 3. The consistency between data of P and R branches indicates

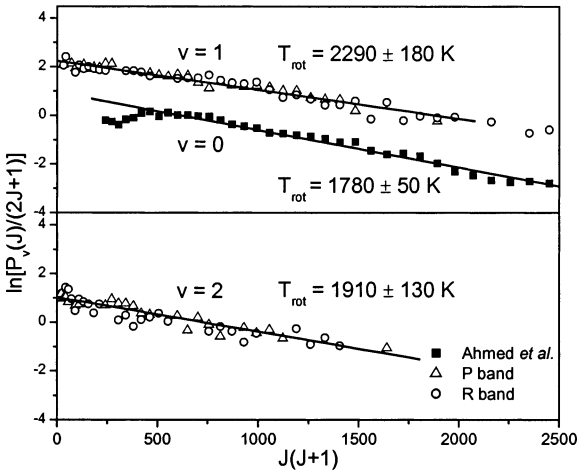

Figure 3. Semilogarithmic plots of relative rotational populations of CO ($v' = 1$ and 2) upon photolysis of $(ClCO)_2$ at 248 nm. Symbols Δ are from P lines and ○ are from R lines; data reported by Ahmed et al. (ref 6; symbols ■) for $v = 0$ are also shown (displaced downward) for comparison. Solid lines represent least-squares fits.

excellent quality of our data and accurate calibration of our instrumental response function. Deduced rotational temperatures are 2290 ± 100 and 1910 ± 130 K for $v' = 1$ and 2, respectively. We also estimated the rotational distribution of CO ($v = 0$) from Figure 5b of Ahmed et al.[6] and plotted it in Figure 3 (symbol ■) for comparison; our result of 2290 K is slightly greater than the rotational temperature of 1780 ± 50 K derived from their data with $J' > 20$. The discrepancy might result from a contribution of "cold" CO in the $v = 0$ state in their experiments; these cold CO molecules are produced from secondary dissociation of ClCO product.

Energetically, with a maximal vibration−rotational excitation energy ~7189 cm^{-1} observed for CO ($v' = 2$, $J' = 39$), the $v' = 3$ level is expected to be populated up to $J \sim 20$, but lines associated with $v' = 3$ cannot be positively identified because other lines overlap and because intensity is small. In one experiment at 0.13 cm^{-1} resolution, we indeed found weak lines ascribable to emission from $v' = 3$ and $J' = 1-8$, but the poor signal-to-noise ratio precludes quantitative analysis. An energy limit of 7189 cm^{-1} corresponds to levels up to $J' = 51$ for $v' = 1$, consistent with our observation of the R(51) line. We calculate relative populations of rotational levels associated with unobserved or overlapped lines according to a Boltzmann distribution. Rotational energies $E_{rot}(v)$ for each vibrational level, obtained on summing a product of level energy and normalized population of each rotational level, are listed in Table 1. A sum

TABLE 1: Rotational Temperature (T_{Rot}), Rotational Energy (E_{Rot}), and Vibrational Population of CO (v) upon Photolysis of $(ClCO)_2$ at 248 nm

v	T_{rot}/K	$\sum_J P_v(J)$[a]	E_{rot}/kJ mol^{-1}	population
0				0.692[b]
1	2290 ± 100	7597	16.5	0.242
2	1910 ± 130	1786	11.8	0.057
3				0.009[b]

[a] $P_v(J)$ = (relative integrated emittance)/[(instrumental response factor)(Einstein coefficient)]; arbitrary unit. [b] Estimated from surprisal analysis; see text.

of relative rotational population in each vibrational state is listed in column $\sum_J P_v(J)$ of Table 1; the ratio gives a relative vibrational population. A rotational energy of 15.6 kJ mol^{-1} averaged over $v' = 1$ and 2 is derived on multiplying $E_{rot}(v)$ from observed data by its corresponding vibrational population. Considering possible experimental errors, we report an average rotational energy of 16 ± 2 kJ mol^{-1} for CO observed in this work. This value is slightly greater than, but within experimental uncertainties of, a value 14.2 kJ mol^{-1} derived from REMPI spectra of CO ($v = 0$).[6]

B. Vibrational Distribution of CO. On the basis of an observed vibrational distribution for $v' = 1$ and 2, we estimate by surprisal analysis the populations of $v' = 0$ and $v' \geq 3$ relative to those of $v' = 1$ and 2. The vibrational distribution of CO normalized for $v' = 0-3$ is shown in Table 1. The average vibrational energy of CO thus derived is 9.8 kJ mol^{-1}. Considering possible errors in estimating population of CO ($v' = 0$), we report an average vibrational energy of 10 ± 3 kJ mol^{-1} for CO observed in this work.

Ahmed et al.[6] reported that the total integrated intensity of the (1−1) band of CO was less than 5% that of the (0−0) band in their REMPI spectra;[6] a zero vibrational energy for CO was used in their energy balance. Our results show that vibrational states of CO with v up to 3 are populated; our estimate of the population of $v' = 1$ is ∼35% that of $v = 0$. The average vibrational energy of CO is thus greater than that deduced from previous measurements. The discrepancy might be due to the predissociative character of intermediate states of CO ($v' > 1$) before ionization in the REMPI scheme; a significant portion of vibrationally excited CO might have escaped direct detection.

C. Energy Balance and Mechanism of Photodissociation. Standard enthalpies of formation at 298 K are −335.8 ± 6.3 kJ mol^{-1} for $(ClCO)_2$,[19] −21.8 ± 2.5 kJ mol^{-1} for ClCO,[20] 121.3 kJ mol^{-1} for Cl, and −110.53 kJ mol^{-1} for CO.[21] Standard enthalpies of reaction for the following channels are

$$(ClCO)_2 \rightarrow ClCO + ClCO \quad \Delta H^0 = 292.2 \text{ kJ mol}^{-1} \quad (1)$$

$$(ClCO)_2 \rightarrow ClCO + Cl + CO \quad \Delta H^0 = 324.8 \text{ kJ mol}^{-1} \quad (2)$$

$$ClCO \rightarrow Cl + CO \quad \Delta H^0 = 32.6 \text{ kJ mol}^{-1} \quad (3)$$

Enthalpies change for reactions 1 and 2 may have errors as large as 9 kJ mol^{-1} because of uncertainties in enthalpies of formation of $(ClCO)_2$ and ClCO.

Ahmed et al.[6] proposed that on photolysis $(ClCO)_2$ undergoes an impulsive three-body dissociation (reaction 2) to form Cl, CO, and ClCO, followed by further decomposition of internally excited ClCO into Cl and CO. Performing a crude calculation of energy balance based on their experimental results, they found that the total energy, including bond-dissociation energies and translational, rotational, and electronic energies of all fragments, sums to 535 kJ mol^{-1}, 26 kJ mol^{-1} greater than an excitation energy of 509 kJ mol^{-1} corresponding to photons at 235 nm.

TABLE 2: Energy Balance (in kJ mol^{-1}) on Photolysis of $(ClCO)_2$ at 248 nm

description	energy	adjustment for thermal energy[a]	balance
Primary Step: Three-Body Dissociation			
photoexcitation energy	482.3		482.3
C−C and C−Cl bond fission, rxn. 2	−324.8		157.5
E_{trans} of fast Cl (ref 6)	−47.2	+3.7	114.0
E_{trans} of fast CO (ref 6)	−30.3	+3.7	87.4
E_{trans} of ClCO (ref 7)[b]	−3.7	+3.7	87.4
E_{rot} of fast CO (this work)[c]	−16	+2.5	73.9
E_v of fast CO ($v \leq 3$) (this work)[c]	−10	+0.0	63.9
resultant E_{int} of ClCO			64
Secondary Step: ClCO Decomposition			
E_{int} of ClCO	63.9	−3.7	
E_{trans} of ClCO (ref 7)[b]	3.7	−3.7	60.2
C−Cl bond fission, rxn. 3	−32.6		27.6
E_{trans} of slow Cl (ref 7)[d]	−14.5	+3.7	16.8
E_{trans} of slow CO (ref 7)[d]	−10.7	+3.7	9.8
E_{int} of slow CO	∼10		

[a] Because available enthalpies of reaction are at 298 K, thermal energies of reactants and products need to be taken into account; see text. [b] Based on results of photolysis at 193 nm with photofragment translational spectroscopy (ref 7) and taking into account that ClCO with small translational energy decomposes; see text. [c] Reference 6 reported E_{rot} = 14.2 kJ mol^{-1} and $E_v = 0$. [d] Based on results of ref 7; see text.

We combined the internal energy of CO determined in this work with translational energies determined previously[6,7] to derive a revised energy balance for photodissociation of $(ClCO)_2$ at 248 nm, as listed in Table 2. Because available enthalpies of reaction apply to 298 K, thermal energies of reactants and products should be taken into account in energy balance. More specifically, thermal energies of products are added, whereas those of reactant are subtracted in calculation of the balance of available energy. After breakage of the C−C and C−Cl bonds, the excess energy is ∼158 kJ mol^{-1} plus thermal energies of products. The total translational energy of Cl, CO, and ClCO amounts to 81.2 kJ mol^{-1}, and the internal energy of CO determined in this work is 26 kJ mol^{-1}; consequently, the average internal energy of ClCO before further decomposition is about 64 kJ mol^{-1}. The average translational energy of surviving ClCO upon photolysis at 193 nm was determined with fragment translational spectroscopy to be 4.6 kJ mol^{-1}.[7] Because about 64% of ClCO decomposes before detection, we estimate that the average translational energy of ClCO before decomposition is thermal (3.7 kJ mol^{-1}).

An average translational energy of slow Cl, 14.5 kJ mol^{-1}, determined with fragment translational spectroscopy upon photolysis at 193 nm,[7] is used because in imaging experiments the rapid component of Cl appears to be underestimated from deconvolution of kinetic-energy profiles pertaining to slow and rapid Cl ($^2P_{3/2}$);[6] the average energy (22.1 kJ mol^{-1}) thus determined for the slow component of Cl is consequently greater than expected. Similarly, the translational energy of the slow CO determined from photofragment translational spectroscopy upon photolysis at 193 nm, 10.7 kJ mol^{-1}, is used because in REMPI experiments the overall distribution was not measured. We expect translational energies of slow Cl and CO produced from photodissociation of $(ClCO)_2$ at 193 nm to be similar to those at 248 nm because dissociation likely takes place on the ground electronic surface of ClCO. In this second stage of dissociation, product Cl carries more kinetic energy than that

of CO because Cl is forward scattered with respect to the motion of ClCO parent.

ClCO with average internal energy about 64 kJ mol^{-1} is unstable because C−Cl bond fission takes only 32.6 kJ mol^{-1}. After taking into account translational energies of Cl and CO, the energy balance leaves about 10 kJ mol^{-1} for the average internal energy of the slow CO, too small to populate substantially the $v = 1$ level but consistent with the rotational distribution of CO ($v = 0$) previously observed with REMPI; in the REMPI experiments, slow CO was observed at $v = 0$, $J = 22$ ($E = 11.6$ kJ mol^{-1}).[6] The infrared emission that we observed likely results entirely from translationally rapid CO molecules produced in the initial step.

The discrepancy of previous calculations of energy balance arises partly from a greater $\Delta H°$ value of 347.0 kJ mol^{-1} for reaction 2 used previously and partly from a large average translational energy of 30 kJ mol^{-1} used for CO (both slow and rapid). According to previous experiments,[6] the average translational energy of CO ($v = 0$, $J = 55$) is 30.3 kJ mol^{-1}, but drops to 12.3 kJ mol^{-1} for CO ($v = 0$, $J = 22$). The vibrational energy of rapid CO (10 kJ mol^{-1}) was also taken as zero in previous report.

In summary, the energy balance is consistent with the two-step mechanism for photodissociation of $(ClCO)_2$ at 248 nm proposed previously.[6,7] The initial step involves three-body decomposition into translationally rapid Cl and CO and slow ClCO; CO produced in this step is highly rotational excited with vibrational excitation up to $v = 3$. Product ClCO is also highly internally excited, so that a large fraction of ClCO further decomposes to form slow Cl and CO; most CO produced in this step is in its vibrational ground state with small rotational excitation, undetectable with our technique.

It should be noted that, in order to produce translationally rapid Cl and CO and slow ClCO in the first step, Cl and CO should depart in almost equal and opposite directions and impart little translational kick to ClCO. It is unclear if this scheme actually takes place. Perhaps the energy balance for photolysis at 193 nm will provide a more stringent test for this mechanism. Measurements of internal energies of CO produced upon photolysis of $(ClCO)_2$ at 193 nm are in progress.

We have identified in IR absorption spectra the C−O stretching (ν_1) mode of ClCO produced from reaction of Cl + CO in our previous work,[22] but we observed no emission of ClCO near 1880 cm^{-1} in this work, indicating that either ClCO ($\nu_1 = 1$) decomposes rapidly or little ClCO ($\nu_1 = 1$) was produced in this work. A small fraction of surviving ClCO is expected to have an internal energy smaller than the bond energy of 32 kJ mol^{-1}. This energy is sufficient to populate the $\nu_1 = 1$ level ($\sim$22 kJ mol^{-1}) of the C−O stretching mode, but most vibrational excitation is likely associated with low-energy modes rather than with CO stretching. The two small vibrational wavenumbers, calculated to be 581 and 340 cm^{-1},[22,23] lie beyond our detection limits.

Conclusion

Rotationally resolved emission from CO up to $v' = 3$ is observed upon photolysis of $(ClCO)_2$ at 248 nm; average rotational and vibrational energies of CO are 16 ± 2 and 10 ± 3 kJ mol^{-1}, respectively. Our results combined with those from photofragment imaging and photofragment translational spectroscopy are consistent with a two-step photolysis scheme of $(ClCO)_2$ proposed previously. The first step yields highly rotationally excited CO fragments with vibrational excitation up to $v = 3$. Most CO produced in secondary decomposition of ClCO is in its vibrational ground state with small rotational excitation; hence, no emission of CO from the secondary step was observed. We observed no emission of ClCO near 1880 cm^{-1}, indicating that surviving ClCO has little vibrational excitation in the CO stretching mode. A revised energy balance fits well with existing enthalpies of formation.

Acknowledgment. We thank the National Science Council of Taiwan (grant no. NSC91-2119-M-007-003) and MOE Program for Promoting Academic Excellence of Universities (Grant No. 89-FA04-AA) for support.

References and Notes

(1) Baklanov, A. V.; Krasnoperov, L. N. *J. Phys. Chem. A* **2001**, *105*, 97.

(2) Hassett, D. M.; Hedberg, K.; Marsden, C. *J. Phys. Chem.* **1993**, *97*, 4670.

(3) Danielson, D. D.; Hedberg, L.; Hedberg, K.; Hagen, K.; Traetteberg, M. *J. Phys. Chem.* **1995**, *99*, 9374.

(4) Durig, J. R.; Davis, J. F.; Wang, A. *J. Mol. Struct.* **1996**, *375*, 67.

(5) Schroeder, W.; Monnier, M.; Davidovics, G.; Allouche, A.; Verlaque, P.; Pourcin, J.; Bodot, H. *J. Mol. Struct.* **1989**, *197*, 227.

(6) Ahmed, M.; Blunt, D.; Chen, D.; Suits, A. G. *J. Chem. Phys.* **1997**, *106*, 7617.

(7) Hemmi, N.; Suits, A. G. *J. Phys. Chem. A* **1997**, *101*, 6633.

(8) Yeh, P.-S.; Leu, G.-H.; Lee, Y.-P.; Chen, I-C. *J. Chem. Phys.* **1995**, *103*, 4879.

(9) Lin, S.-R.; Lee, Y.-P. *J. Chem. Phys.* **1999**, *111*, 9233.

(10) Lin, S.-R.; Lin, S.-C.; Lee, Y.-C.; Chou, Y.-C.; Chen, I-C.; Lee, Y.-P. *J. Chem. Phys.* **2001**, *114*, 160.

(11) Lin, S.-R.; Lin, S.-C.; Lee, Y.-C.; Chou, Y.-C.; Chen, I-C.; Lee, Y.-P. *J. Chem. Phys.* **2001**, *114*, 7396.

(12) Wu, C.-Y.; Chung, C.-Y.; Lee, Y.-C.; Lee, Y.-P. *J. Chem. Phys.* **2002**, *117*, 9785.

(13) Huang, Y.; Yang, Y. A.; He, G. X.; Hashimoto, S.; Gordon, R. J. *J. Chem. Phys.* **1995**, *103*, 5476.

(14) Reilly, P. T. A.; Xie, Y.; Gordon, R. J. *Chem. Phys. Lett.* **1991**, *178*, 511.

(15) Huang, Y.; Yang, Y. A.; He, G. X.; Gordon, R. J. *J. Chem. Phys.* **1993**, *99*, 2752.

(16) Huang, Y.; Gordon, R. J. *J. Chem. Phys.* **1997**, *106*, 1418.

(17) Ogilvie, J. F.; Cheah, S.-L.; Lee, Y.-P.; Sauer, S. P. A. *Theor. Chem. Acc.* **2002**, *108*, 85.

(18) Ogilvie, J. F. *The Vibrational and Rotational Spectrometry of Diatomic Molecules*; Academic Press: London, 1998.

(19) Walker, L. C.; Prophet, H. *Trans. Faraday Soc.* **1967**, *63*, 879.

(20) Nicovich, J. M.; Kreutter, K. D.; Wine, P. H. *J. Chem. Phys.* **1990**, *92*, 3539.

(21) Atkinson, R.; Baulch, D. L.; Cox, R. A.; Hampson, R. F., Jr.; Kerr, J. A.; Troe, J. *J. Phys. Chem. Ref. Data* **1989**, *18*, 881.

(22) Chen, S.-H.; Chu, L.-K.; Chen, Y.-J.; Chen, I-C.; Lee, Y.-P. *Chem. Phys. Lett.* **2001**, *333*, 365.

(23) Schnöckel, H.; Eberlein, R. A.; Plitt, H. S. *J. Chem. Phys.* **1992**, *97*, 4.